J. exp. Biol. 156, 287–314 (1991)
Printed in Great Britain © *The Company of Biologists Limited 1991*

HYDRODYNAMICS OF RAPID SHELL CLOSURE IN ARTICULATE BRACHIOPODS

BY SPAFFORD C. ACKERLY*

Department of Geological Sciences, Cornell University, Ithaca, NY 14853, USA

Accepted 5 October 1990

Summary

The rapid shell-closing mechanism in articulate (hinged) brachiopods is subject to important hydrodynamic constraints related to expulsion of water from the shell. Fluid forces influence, for example, the speeds of shell closure and the mass flux rates of water from the shell. The principal hydrodynamic forces acting on a shell during rapid closure are (1) inertial reactions, due to the acceleration of water (=acceleration reaction), and (2) water pressure forces which develop as water is expelled from the shell. A generalized hydrodynamic model describes the relative magnitudes of the acceleration and pressure forces as functions of the shell's angular acceleration, velocity and gape. In general, the acceleration reaction dominates the kinematics of shell closure during the initial phases of a closing event, whereas pressure forces dominate towards the later phases of shell closure. Solutions of the general model predict how variables such as the closing speed and the mass flux of water depend on shell size, initial shell gape and on the magnitude of the closing force. Results indicate that inertial reactions (due to acceleration of water) dominate the mechanics of shell closure in articulate brachiopod taxa.

Introduction

Articulate brachiopods are sessile, suspension-feeding organisms, with a shell either free-lying on the sea floor, or fixed to the substratum by a fleshy pedicle or by cementation. A brachiopod's repertoire of skeletal motions is restricted to a few movements of the shell, including rapid shell closure by a twitch contraction of the 'quick' adductor muscles (Rudwick, 1961; Wilkens, 1978*a*) (Fig. 1). Rapid shell closure serves several functions, including (1) protection from predators (brachiopod predation is documented in Paleozoic taxa), (2) protection from environmental adversities, such as turbidity, salinity or exposure to air, (3) expulsion of detritus, feces and gametes from the shell, and (4) reorientation of the shell in free-lying taxa (e.g. Rudwick, 1961). In general, the performance of the closing mechanism depends on the ability to achieve high closing speeds of the

* Present address: Department of Geology, University of Glasgow, Glasgow G12 8QQ, UK.

Key words: brachiopods, hydrodynamics, functional morphology, constraint, *Terebratalia transversa*.

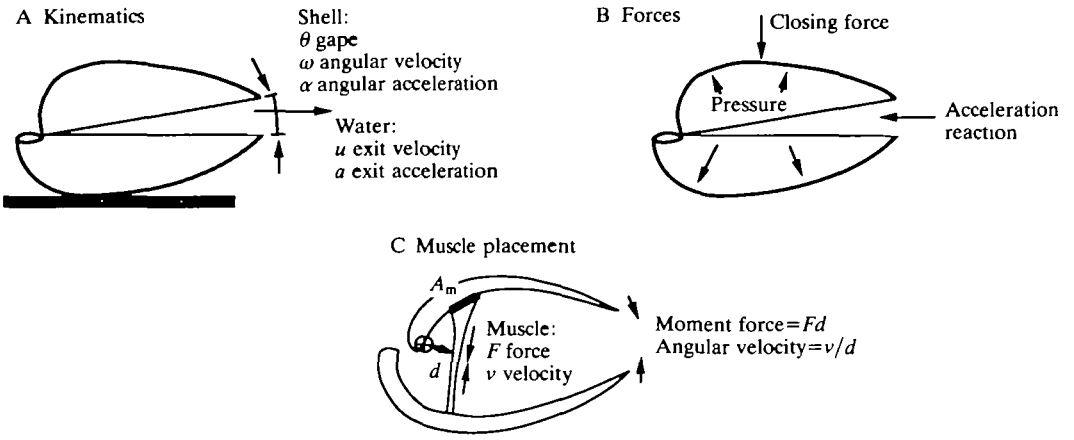

Fig. 1. Diagram of the brachiopod shell showing (A) the kinematic parameters, (B) the forces involved in closure, and (C) the 'quick' adductor muscle position. d, moment arm distance; A_m, cross-sectional area of muscle base.

shell, utilizing a rapid twitch contraction of the closing muscles. Rapid closing speeds increase the rate of mass flux of water for expelling material from the shell and also enhance the protective value of the closing mechanism. There are, however, fundamental mechanical constraints on the attainable rates of shell closure, related to both (1) the physiological properties of the muscle contractile tissues, and (2) the nature of the hydrodynamic reactions as water is expelled from the shell. This paper addresses the hydrodynamic properties of rapid shell closure (muscle properties will be discussed in a subsequent paper; S. C. Ackerly, in preparation). What are the hydrodynamic forces acting on a rapidly closing shell? In what ways have hydrodynamic forces influenced the evolution of the rapid shell-closing mechanism? Are there upper limits to the speeds of shell closure or to size based on hydrodynamic considerations? Hydrodynamic principles are explored using a variety of 'shell' structures, including idealized flat plate models with simple geometries and actual shells of brachiopods.

Hydrodynamic principles

There are two important hydrodynamic forces acting on a rapidly closing shell, be it a bivalved shell, a shell model or two flat plates. The first is related to the acceleration of water surrounding the shell and is the acceleration reaction (Daniel, 1983, 1984); the second is related to the development of water pressure inside the shell. The acceleration reaction describes the forces necessary to accelerate, or decelerate, a certain mass of water in the vicinity of the shell as the shell closes. The so-called 'added mass' of the water plus the mass of the shell (and any tissues) constitute the total inertia of the system (the m in Newton's $F=ma$, where F is force, m is mass and a is acceleration). The second force, that due to water pressure, is related to the exit velocity of water leaving the shell. As the shell

closes, water is forced out of an increasingly small gap in the shell margin, and there is a corresponding pressure rise inside the shell. The pressure gradient across the shell margin and the exit velocity of water from the shell are related by the Bernoulli equation (pressure$\propto$velocity^2).

In general, the initial phases of shell closure are dominated by inertial considerations, when accelerations are high and water exit velocities are relatively low. Pressure forces, in contrast, tend to dominate towards the end of a closing event, when shell closing velocities are high and shell gapes are small. This analysis attempts to define the relative magnitudes of the acceleration and pressure forces, and to determine how these forces are related to shell size, initial shell gape and closing speed.

The quantitative analysis of shell closure follows from Newton's third Law, $\Sigma F=ma$, or

$$\text{closing forces} - \text{pressure forces} = ma, \tag{1}$$

where the closing forces are due to gravity (in the models) or muscles (in organisms), and the mass m and acceleration a refer to the masses and accelerations of the shell and surrounding water. According to equation 1, the system accelerates when the closing forces exceed the internal pressure forces, and decelerates when the opposite is true. The principal difficulties of determining the magnitudes of the hydrodynamic forces acting *in situ* in living brachiopods are (1) most brachiopods are small, of the order of one to several centimeters, and the corresponding forces are small; (2) shell closure is rapid, with durations of the order of tens to hundreds of milliseconds; and (3) the muscle forces and the hydrodynamic forces are non-steady and highly transient. Because of these inherent difficulties, the present analysis uses empty shells and shell models to determine the hydrodynamic properties of shell closure. In the models the closing forces are due to gravity, and friction and other 'external' forces are assumed to be negligible (see below).

In this analysis, the hydrodynamic forces are determined by a combination of empirical measurements and theoretical calculations. In the empirical work I applied known forces to close the shell models, and then calculated the magnitudes of the pressure and inertial forces by fitting equation 1 to the data on closing speeds observed in the models. Solutions of the hydrodynamic model were then generalized in order to predict the velocity of shell closure, given the initial starting conditions (shell size, closing forces and initial gape).

Mechanics of shell closure

For a shell rotating about a fixed hinge axis (a reasonable approximation in this instance), the angular equivalent of Newton's third Law is:

$$\Sigma M = I\alpha, \tag{2}$$

where ΣM is the sum of the moment forces acting on the system, I is the system's moment of inertia and α is the angular acceleration. A moment force is a force F

acting at some distance d from the hinge axis, or fulcrum, so that $M=Fd$. The inertia I is the angular equivalent of mass.

The principal moment forces acting on the shell model are the gravitational closing forces M_g and the water pressure forces M_p (Fig. 1), so that:

$$\Sigma M = M_g + M_p . \tag{3}$$

The system's inertia consists of one component due to the shell's mass I_b, and one component due to the added mass of water I_l. The right-hand term in equation 2 becomes:

$$I\alpha = I_b\alpha + I_l a_l , \tag{4}$$

(the subscripts b and l stand for body and liquid, respectively). Combining equations 2–4 gives the model:

$$M_g + M_p = I_b\alpha + I_l a_l . \tag{5}$$

Gravitational closing forces

The closing forces are due to gravity, acting both on the shell mass m_b and the mass of any external loads m_f, such as the velocity transducer which measures the closing event ($M_g=M_b+M_f$). The weight of the shell $m_b g$, where g is the acceleration due to gravity, is acting at the center of mass of the shell, located at $k_{cm}L$, where k_{cm} is a coefficient and L is the shell length, so that the moment due to gravity is:

$$M_b = m_b g k_{cm} L . \tag{6}$$

The shell mass may be expressed as:

$$m_b = (\rho_b - \rho_l)V_b , \tag{7}$$

where ρ_b is the density of the shell material, ρ_l is the fluid density and V_b is the volume of shell material. Volume may be expressed as:

$$V_b = k_w k_t L^3 , \tag{8}$$

where k_w is a width coefficient (see equation 12) and k_t a thickness coefficient (the coefficients k are derived in the Appendix). Combining equations 6–8 gives:

$$M_b = (\rho_b - \rho_l)k_w k_t k_{cm} g L^4 . \tag{9}$$

The gravitational forces of external loads are:

$$M_f = m_f(g - a_f)d_f , \tag{10}$$

where d_f and a_f are, respectively, the position of the load with respect to the hinge and the downward linear acceleration of the load. The load is uncoupled from the shell and hence produces zero force on the shell in a free fall (where $a_f=g$). The moment forces due to gravity are known quantities in the analysis, and are readily measured or derived.

Pressure forces

The pressure in the shell P (pressure=force per unit area) is acting upon the internal shell surface area A_s to produce a pressure force equal to A_sP. The pressure force is taken to act at the center of pressure, at a distance $k_{cp}L$ from the hinge axis, to produce a pressure moment M_p, where:

$$M_p = A_sPk_{cp}L\,. \tag{11}$$

The surface area A_s is related to shell length by:

$$A_s = k_wL^2\,. \tag{12}$$

From Bernoulli's equation, the pressure is related to the mean exit velocity of water from the shell u_l by:

$$P = C_p{}^*\rho_l u_l{}^2/2\,, \tag{13}$$

where $C_p{}^*$ is a pressure coefficient. $C_p{}^*$ is related to the Reynolds number, where the length term is the width of the shell gape (θL, where θ is the gape) and the velocity term is the exit velocity of water from the shell u_l:

$$Re = \theta Lu_l/\nu\,, \tag{14}$$

where ν is the kinematic viscosity of water.

The mean water exit velocity is related to the rate of change of internal shell volume dV/dt and to the area of the gape at the shell margin A_{ex} by:

$$u_l = (dV/dt)/A_{ex}\,. \tag{15}$$

The volume derivative dV/dt is:

$$dV/dt = k_ak_wL^3\omega\,, \tag{16}$$

where k_a is a coefficient of the first moment of area (see Appendix). The exit area A_{ex} is:

$$A_{ex} = k_{ex}L^2\theta\,, \tag{17}$$

where k_{ex} is a coefficient of the first moment of the shell's perimeter (see Appendix). ω and θ are the instantaneous values of the shell's angular velocity and gape. Combining equations 15–17 gives the mean exit velocity of water u_l as:

$$u_l = k_ak_wL\omega/k_{ex}\theta\,. \tag{18}$$

The expression for the pressure moment becomes:

$$M_p = \rho_lC_p{}^*k_{cp}k_wu_l{}^2L^3/2 \tag{19}$$

or, by substitution of equation 18,

$$M_p = \rho_lC_pk_a{}^2k_w{}^3L^5\omega^2/2k_{ex}{}^2\theta^2\,, \tag{20}$$

where $C_p=C_p{}^*k_{cp}$. The pressure moment depends directly on the square of the shell's closing velocity and inversely on the square of the shell's gape ($M_p\propto\omega^2/\theta^2$). The coefficient C_p is the only unknown in equation 20.

The shell's inertia

The standard equation for the moment of inertia I_b of a body is:

$$I_b = J_b m_b L^2, \tag{21}$$

where J_b is an inertia coefficient, m_b is the mass of the body and L is the length of the body. Substituting equations 7 and 8 into equation 21 gives the shell's inertia as:

$$I_b = J_b \rho_b k_w k_t L^5, \tag{22}$$

showing that the angular inertia (mass) is proportional to the fifth power of shell length. All of the coefficients in equation 22 can be measured or calculated.

Inertia due to water

The added mass of water surrounding a thin plate may be taken as (Saunders, 1957):

$$I_l = J_l \rho_l L^5, \tag{23}$$

where J_l is the coefficient of inertia of the water and ρ_l is the fluid density. Saunders (1957) gives a value of 0.178 for the added inertia of a thin semi-circular plate. An alternative expression for I_l is:

$$I_l = \gamma J_b \rho_l V_b L^2, \tag{24}$$

where γ is the added mass coefficient, or the proportion of a body's inertia attributable to the surrounding water (equation 24 is the angular equivalent of the linear form: $I_l = \gamma \rho_l V_b$). Equation 24 is not, however, useful for very thin plates where the body's mass is negligible in comparison to the added mass of the water.

This analysis adopts the expression in equation 23, but relates the water's inertia to the mean acceleration of water leaving the shell, rather than to the acceleration of the body (in a similar fashion, pressure was related to the exit velocity of water from the shell and not to the shell's velocity). The mean exit acceleration a_l, substituting α for ω in equation 18, is:

$$a_l = k_a k_w L \alpha / k_{ex} \theta. \tag{25}$$

Thus, the inertia term for the water mass $I_l a_l$ becomes:

$$I_l a_l = J_l \rho_l k_a k_w L^6 \alpha / k_{ex} \theta. \tag{26}$$

J_l, the coefficient of fluid inertia is, an unknown in the analysis.

It should be noted that the use of the water's exit acceleration rather than the shell's acceleration introduces a unit discrepancy in this moment force term (units become N m^2, rather than N m). In an isometric system, the term also scales as L^6 rather than L^5. The rationale for this choice is that using the water's exit acceleration provides a better empirical fit of the model to the data than using the shell's acceleration.

Solution of the hydrodynamic equations

The differential equation describing the hydrodynamics of shell closure is, from the equations above:

$$K_1\alpha + K_2\alpha/\theta + K_3\omega^2/\theta^2 + K_4 = 0\,, \tag{27}$$

where K_1 is a coefficient of shell acceleration:

$$K_1 = J_b\rho_b k_w k_t L^5\,, \tag{28}$$

K_2 is a coefficient of fluid acceleration:

$$K_2 = J_l\rho_l k_a k_w L^6/k_{ex}\,, \tag{29}$$

K_3 is a coefficient of pressure:

$$K_3 = \rho_l C_p k_a{}^2 k_w{}^3 L^5/2k_{ex}{}^2 \tag{30}$$

and K_4 is the magnitude of external forces on the shell:

$$K_4 = -(\rho_b - \rho_l)k_w k_t k_{cm} g L^4 - m_f d_f g\,. \tag{31}$$

Strictly speaking, the second term in the equation for $K_4(m_f d_f g)$ should be corrected for the shell's acceleration, but the correction is small and can be neglected.

The only unknown terms in equation 27 are the coefficient of fluid inertia J_l and the pressure coefficient C_p. J_l may be found by solving equation 27 at time $t=0$ when the pressure force (third term in equation 27) is approximately zero ($\omega\approx 0$). C_p may be found by solving equation 27 at the time of maximum velocity, $t_{\omega max}$, when the shell's acceleration is zero (for $\alpha=0$, the first two terms in equation 27 equal zero).

In this analysis, equation 27 has been solved by a simple stepwise numerical algorithm (Euler's method) where the starting condition is the initial gape θ_0, and where the initial velocity and acceleration are zero ($\omega_0=\alpha_0=0$) (the Runge–Kutta method gives very similar results). The step length was set so that a solution was obtained in 75–250 steps. Equation 27 appears to be well-behaved under most conditions (except at high closing forces); variation in step length within the above bounds had no noticeable effect on the solution.

Once J_l and C_p have been established for a particular shell morphology, equation 27 can be used to predict the hydrodynamic behavior of the shell-closing system. We may ask how closing speeds are related to external forces on the shell, to changes in size, or to changes in the initial shell gape. What are the disadvantages, if any, of large size or high speeds? Are hydrodynamic forces an important constraint on the design of a rapid shell-closing system?

Mass flux of water – mean thrust

The brachiopod's ability to expel material (e.g. gametes, detritus) from the shell should be related to the mass flux of water from the shell (thrust, in many situations moves the animal; here the animal is stationary and the water moves). A

calculation of the thrust produced during shell closure should provide an estimate of the capacity to entrain material in water leaving the shell. Thrust (units of force) is the product of the mass flux dM/dt and the exit velocity of the fluid u_l:

$$T = u_l dM/dt. \tag{32}$$

Substitution of equations 15 and 16 for the mean fluid exit velocity and the mass flux ($dM/dt = \rho dV/dt$) gives the equation for the thrust:

$$T = K\rho_l L^4 \omega^2/\theta, \tag{33}$$

where $K = k_a^2 k_w^2/k_{ex}$. The thrust force varies during the course of a closing event in proportion to the quantity ω^2/θ. Equation 33 gives the magnitude, but not a direction, for the thrust force. The mean thrust T_m is taken as:

$$T_m = 1/t_c \int^t T dt, \tag{34}$$

where t_c is the closing time and T is the thrust at time t during the interval dt. The mean thrust may be calculated during solution of equation 27.

The efficiency ϵ of the closing moment for the generation of thrust is defined as the ratio of the energy outputs (work done by thrust forces) to energy inputs (work done by the closing forces, i.e. the muscles in living animals, gravity in the models). Energy output E_o is:

$$E_o = \int^t T u_l dt. \tag{35}$$

Energy input E_i is the product of the closing moment M on the shell and the shell gape θ:

$$E_i = M\theta. \tag{36}$$

The thrust force and efficiency of thrust production, calculated by the model, are discussed below.

Methods for measuring shell closure

Models and shells were immersed in water and closing events measured either electronically or strobo-photographically. The brachiopod shells, with tissues removed, were of the species *Terebratalia transversa*. Two types of models were used: (1) semi-circular flat-plate models, and (2) 'brachiopod-like' models hand-molded from the compound Polyform (Fig. 2). The brachiopod shells were mounted by gluing the pedicle (ventral) valve to a plate, and letting the brachial (dorsal) valve rotate freely about the hinge. A trip mechanism, inserted between the two plates or valves, set the initial gape, and rapid removal of the trip rod initiated the closing event. In all cases, the shells closed under their own weight, the weight of the velocity transducer and, in some cases, the weight of additional loads (Fig. 2). The plate models were constructed from 5.7 mm thick Plexiglas. One plate was fixed about 2 cm above the aquarium bottom, and a second plate was hinged to it using a strip of duct tape. Closure occurred as in the empty brachiopod shells.

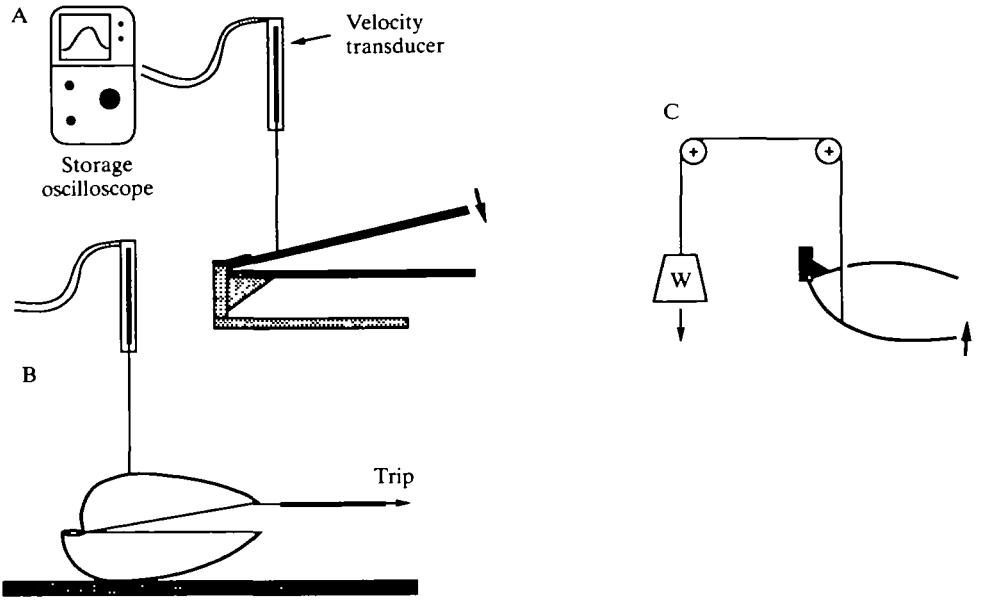

Fig. 2. Experimental apparatus for measurements of shell closure. (A) A velocity transducer is connected to a Plexiglas plate model by a thin wire, with output to an oscilloscope. (B) Same as A, but the transducer is connected to a shell. (C) Models made of Polyform were closed by a wire connected to a weight (W). The position of the shell with time was measured photo-stroboscopically (see text).

Closure in the empty shells and Plexiglas models was measured with a linear output velocity transducer (Trans Tek model 001) with output recorded on a storage oscilloscope (Tektronix model 564B). The voltage output of the transducer was calibrated to the slope of the time–velocity curve of the transducer in free fall (constant slope equal to the acceleration of gravity, $9.8\,m\,s^{-2}$). The transducer was connected to the shell or model by a wire rod resting in a shallow hole in the upper valve, usually about 0.5–1.0 cm from the hinge (Fig. 2A). Linear velocities v recorded by the transducer were transformed to angular velocities ω of the shell by the usual convention $\omega = v/d_f$ where d_f is the position of the transducer relative to the hinge. Tracings from the oscilloscope recordings were digitized and data were analyzed by computer.

In the shells fabricated from Polyform, the valves were articulated by a wire pin. The upper valve was fixed to a frame and the lower valve rotated upwards by a weight fixed to a fine wire running through the upper valve and through a pulley system (Fig. 2C). The wire was connected to a trip mechanism which initiated closure. During closure, valve motions were illuminated by a stroboscope (60–420 flashes s^{-1}), and successive valve positions were recorded photographically.

Results

Figs 3 and 4 show data on the gape, angular velocity and angular acceleration of

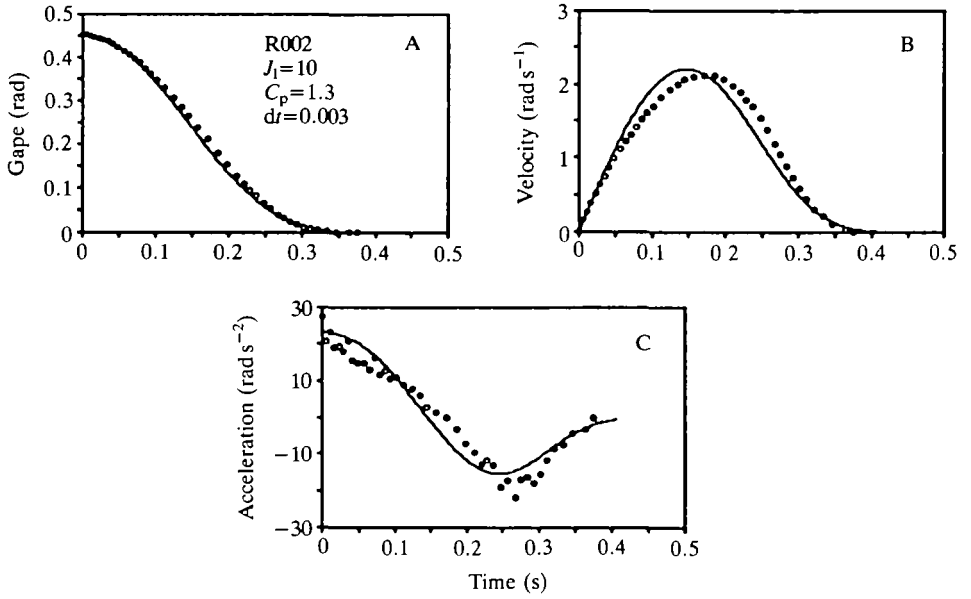

Fig. 3. Kinematic data for a typical Plexiglas model 'shell'-closing event; showing the shell's gape (A), angular velocity (B) and angular acceleration (C) as functions of time. Figures show observations (circles) and predictions of the hydrodynamic model (lines). The 'shell', a semi-circular Plexiglas model, accelerates under a constant load to a maximum velocity part way through the event, and then decelerates due to the development of water pressure within the shell. R002 identifies the event (see Tables 2 and 3), J_1 is the coefficient of fluid inertia, C_p is the pressure coefficient and dt is the time step in seconds for the numerical solution.

a shell model, as functions of time, during typical shell-closing events (Fig. 5 shows additional data on the angular closing velocity in a selection of closing events). The data show rapid accelerations during the initial phases of shell closure, maximum velocities roughly midway through the closing event, and rapid decelerations of the shell as the two valves approach each other. These data on the kinematics of shell closure, together with data on the size and shape of the shells (see Table 1), permit calculations of the hydrodynamic forces involved in a shell-closing event, in particular (1) the mass of water accelerated as the shell speeds up and slows down, and (2) the pressure forces that develop as water is expelled from the shell. These forces may be estimated from solutions of the hydrodynamic model, and the results compared with empirical data.

The coefficients of fluid inertia (J_I) and pressure (C_p)

Values of the coefficients J_1 and C_p, determined for each model closing event, are tabulated in Table 2. The predictions of the hydrodynamic model, using these coefficients, are indicated by solid lines in Figs 3 and 4 and in the plots in the left-hand column of Fig. 5. The model gives a reasonable approximation of the shell's closing history, although there is some variability in the values of the coefficients

determined for different shell-closing events (a closing event refers to a single closing episode). The mean values of J_l and C_p are 10 and 1.5, respectively.

The variability in J_l and C_p can be assessed by solving the model using the mean values of the coefficients, rather than specific values, to see how well the generalized model fits the data. Figs 5 and 6 show the fit between model and data when mean values of the coefficients are used in place of event-specific values. The model often gives a reasonable description of the initial phases of shell closure, but

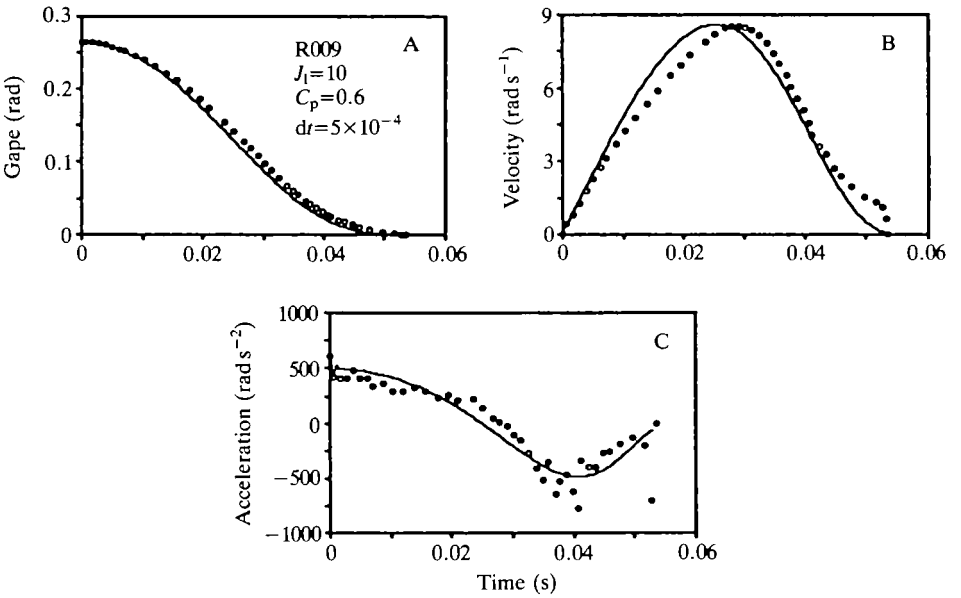

Fig. 4. Kinematic data for a closing event for an empty brachiopod shell (*Terebratalia transversa*) (for further details see Fig. 3 legend).

Table 1. *Size and shape characteristics of the models used in the analysis of shell closure*

	A	B	T	Alice	Fred
k_w	1.57	1.57	1.20	1.20	1.20
k_t	5.7/L*	5.7/L*	0.056	0.056	0.056
J_b	0.250	0.250	0.130	0.130	0.130
k_{cm}	0.424	0.424	0.45	0.45	0.45
k_{ex}	2.00	2.00	1.70	1.70	1.70
k_a	0.424	0.424	0.450	0.450	0.450
L (×10^{-2} m)	4.42	11.1	1.81	4.2	4.6
ρ (×10^{-3} kg m^{-3})	1.21	1.21	2.7	1.8	1.8

A, B, T, Alice and Fred refer to specific models (see text for details).

A, B, semicircular Plexiglas plates (τ=5.7 mm); T, shell of the brachiopod *T. transversa*; Alice, Fred, models molded from Polyform.

* L is the shell length in mm; τ is the shell thickness in mm.

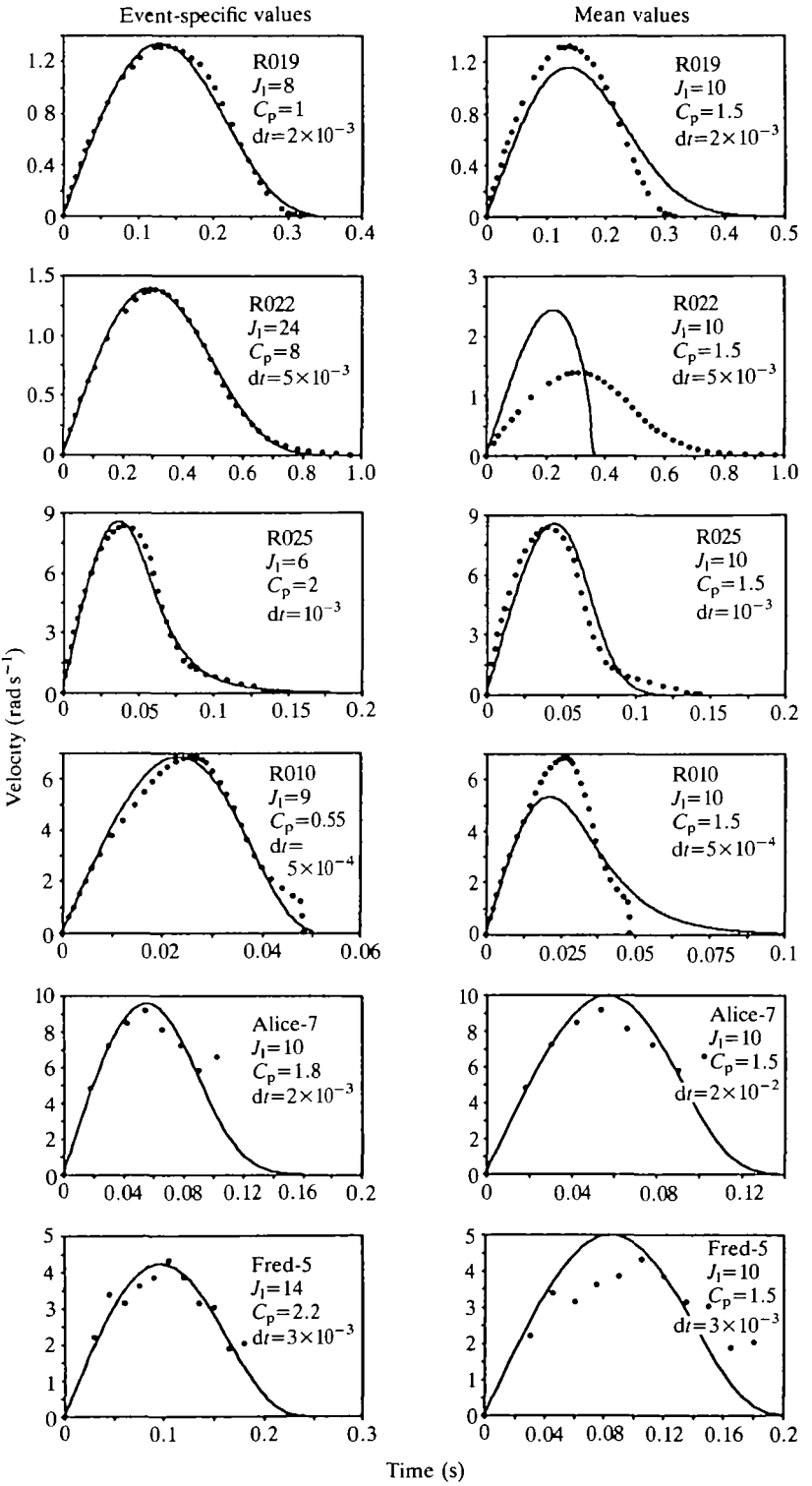
Event-specific values
Mean values
R019
J_1=8
C_p=1
dt=2×10^{-3}
R019
J_1=10
C_p=1.5
dt=2×10^{-3}
R022
J_1=24
C_p=8
dt=5×10^{-3}
R022
J_1=10
C_p=1.5
dt=5×10^{-3}
R025
J_1=6
C_p=2
dt=10^{-3}
R025
J_1=10
C_p=1.5
dt=10^{-3}
R010
J_1=9
C_p=0.55
dt=
5×10^{-4}
R010
J_1=10
C_p=1.5
dt=5×10^{-4}
Alice-7
J_1=10
C_p=1.8
dt=2×10^{-3}
Alice-7
J_1=10
C_p=1.5
dt=2×10^{-2}
Fred-5
J_1=14
C_p=2.2
dt=3×10^{-3}
Fred-5
J_1=10
C_p=1.5
dt=3×10^{-3}
Velocity (rad s^{-1})
Time (s)

Fig. 5

Fig. 5. A comparison of predicted (lines) shell-closing velocities using the event-specific (left column) and mean (right column) values of the hydrodynamic coefficients. Circles represent observations. R019 identifies the event (see Tables 2 and 3), J_1 is the coefficient of fluid inertia, C_p is the pressure coefficient and dt is the time step in seconds for the numerical solution. Also see Fig. 6.

diverges from observations towards the end of a closing event (Figs 5 and 6). For this reason, the half-time of shell closure is a better predictor of the closing event history than is the time for complete closure. In general, it is possible to predict maximum closing velocities and closing times to within 10% of their measured values, using the event-specific values of the coefficients, and to within about 25% using the mean values of these coefficients (Table 3).

The most likely sources of variability in the coefficients J_1 and C_p are hydrodynamic instabilities, experimental error and limitations of the theoretical model. Experimental difficulties are suspected because of variability in results

Table 2. *Values of the hydrodynamic coefficients derived for different models and for different closing events*

Model	Event	θ (rad)	M_s (N m×10⁴)	J_1	C_p	Re_{max}	$I_1a/I_b\alpha$ (rad^{-1})
A	R002	0.453	8.72	10.0	1.3	1.4×10^3	5.3
A	R019	0.240	8.72	8.0	1.0	8.6×10^3	8.0
A	R018	0.239	72.8	5.5	0.6	2.2×10^3	5.5
A	R020	0.236	73.1	5.0	0.65	2.2×10^3	5.1
A	R023	0.369	266.8	12.5	0.2	4.9×10^3	8.1
A	R025	0.483	270.1	6.0	2.0	5.5×10^3	3.0
B	R021	0.303	8.44	3.5	1.0	1.8×10^3	20
B	R022	0.588	2046.9	24.0	8.0*	5.7×10^3	59*
B	R026	0.130	2046.9	1.4	0.6*	4.6×10^3	19
T	R009	0.265	2.76	10.0	0.6	8.9×10^2	11
T	R010	0.199	2.76	9.0	0.55	7.1×10^2	13
Alice	A03	0.687	34.5	12.0	2.0	3.3×10^3	15
Alice	A07	0.719	83.7	10.0	1.8	5.1×10^3	12
Alice	A11	0.688	124.5	10.0	1.5	6.4×10^3	12
Alice	A15	0.646	175.4	7.0	1.6	7.0×10^3	9.2
Fred	F03	0.844	48.1	17.0	3.5	3.6×10^3	19
Fred	F05	0.549	48.1	14.0	2.2	2.9×10^3	24
Fred	F08	0.419	48.1	10.0	1.8	2.3×10^3	22
Means (excluding values marked *):				10.0	1.5		

Data for each closing event include the initial shell gape (θ), and the static closing load (M_s).

The hydrodynamic coefficients are the coefficient of inertia of the fluid (J_1), and the pressure coefficient (C_p).

The maximum Reynolds number (Re_{max}) occurs at the time of the maximum shell closing velocity.

$I_1a/I_b\alpha$ represents the ratio of liquid inertia to body inertia at the initiation of the closing event.

1 g cm=0.98×10^{-4} N m.

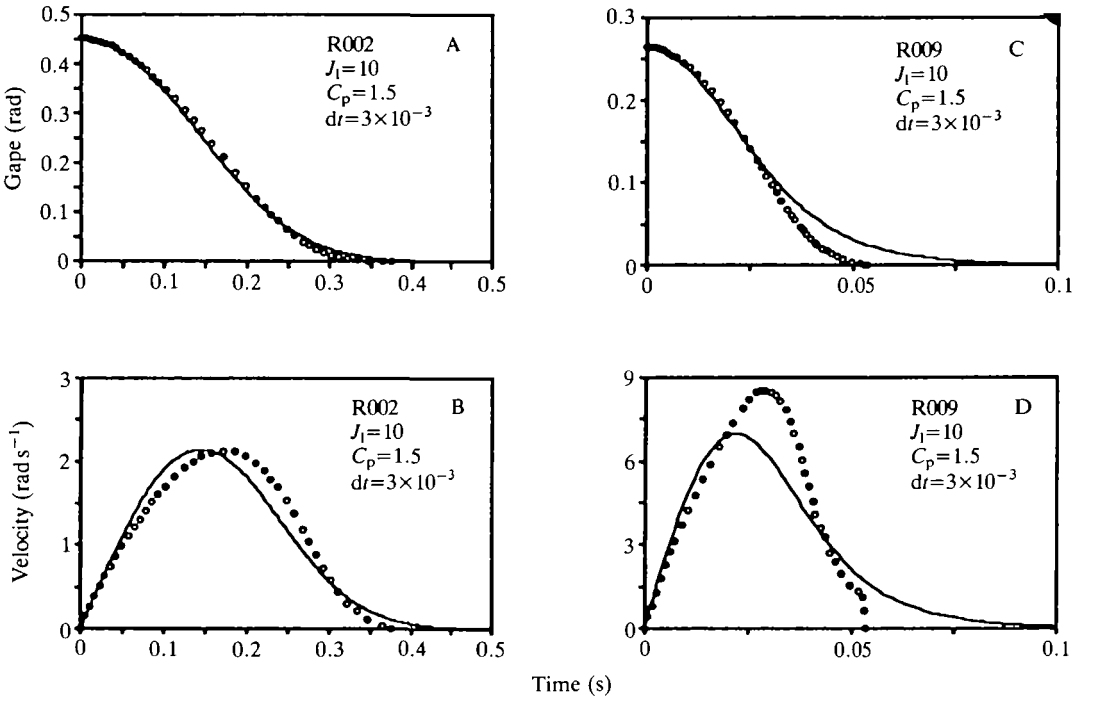

Fig. 6. Comparison of observed (circles) and predicted (lines) shell-closing events using the mean values of the hydrodynamic coefficients (J_I=10 and C_p=1.5) rather than the event-specific values listed in Table 2. (A) Shell gape, event R002. (B) Shell velocity, event R002. (C) Shell gape, event R009. (D) Shell velocity, event R009. Predicted values are reasonably close during the initial phases of the event. R002 identifies the event (see Tables 2 and 3), J_I is the coefficient of fluid inertia, C_p is the pressure coefficient, and dt is the time step in seconds for the numerical solution.

from successive runs on the same models, with the same starting conditions. I believe the difficulty is due to hydrodynamic instabilities that occur at high accelerations and decelerations of the shell. Some variations in the initial starting conditions are also possible, for example if the load orientation is at a small angle from the vertical or if removal of the trip rod causes some vibration or movement of the apparatus. Hydrodynamic instabilities are noted as small velocity oscillations in some of the runs. The instabilities are probably related to shedding of vortices from the valve margins. For example, certain models (large plates, length about 12 cm) were not included in the analysis because of their unsteady behavior while moving through the fluid (strong velocity oscillations).

The hydrodynamic model is apparently not robust at small gapes (see above). This is probably because the model is based on inviscid flow principles where strong boundary layer effects are ignored. However, as the shell gape becomes very small, there are potentially large boundary layer effects on the flow. Violation of these model assumptions perhaps results in the poor fit between model and data observed at small gapes (see above). A statistical analysis of the data in Table 2

Table 3. *Comparison of model predictions with observations*

Event	$\partial_{t1/2}$	$\partial^*_{t1/2}$	$\partial_{\omega max}$	$\partial^*_{\omega max}$
R002	−1.1	−1.1	4.8	1.5
R009	−8.5	−2.9	1.0	−17.9
R010	1.1	14.3	0.4	−22.0
R018	−5.2	21.8	0.8	−26.6
R019	4.4	16.6	1.8	−12.1
R020	−5.6	24.1	0.3	−27.3
R021	−0.0	60.3	−0.5	−33.0
R022	0.4	−35.2	1.2	76.7
R023	17.0	–	2.7	–
R025	1.7	11.6	2.7	2.3
R026	4.7	136.7	2.7	−49.3
A03	4.2	−5.4	8.6	20.8
A07	3.7	3.7	4.7	8.7
A11	8.9	8.9	−1.4	−1.4
A15	14.2	22.8	0.5	−4.2
F03	14.0	−13.0	2.0	38.8
F05	10.0	−6.6	−1.9	15.8
F08	12.0	12.0	9.9	14.1
Means	6.4	23.3	2.7	21.9

The table gives the percentage error in the predicted time for closure of the shell to half the initial gape for event-specific values of the hydrodynamic coefficients J_1 and C_p ($\partial_{t1/2}$), and for mean values of the coefficients ($\partial^*_{t1/2}$), and also the percentage error in the predicted values of the maximum closing velocity, for both event-specific values of the coefficients ($\partial_{\omega max}$), and for mean values of the coefficients ($\partial^*_{\omega max}$).

Specific and mean values of the coefficients are given in Table 2.

The percentage error=100[(predicted value−observed vale)/predicted value].

Mean errors reflect means computed on the errors' absolute values.

shows a weak but significant dependence of the coefficients (J_1 and C_p) on the initial shell gape θ, the closing moment M and the Reynolds number Re. These patterns indicate that the mathematical model does not account for all the variables.

Discussion

Hydrodynamic reactions

The primary forces involved in shell closure are (1) the closing force, which is gravity in the models, (2) the acceleration reaction, or the force required to accelerate the shell and surrounding fluid, and (3) the pressure force, which is related to the velocity of water leaving the shell. The relative magnitudes of these forces, as predicted by the hydrodynamic model, are indicated in Fig. 7 for two closing events.

When a shell closes rapidly (60 ms is roughly the duration of a shell-closing event in the brachiopod *T. transversa*. S. C. Ackerly, in preparation), the hydrodynamic

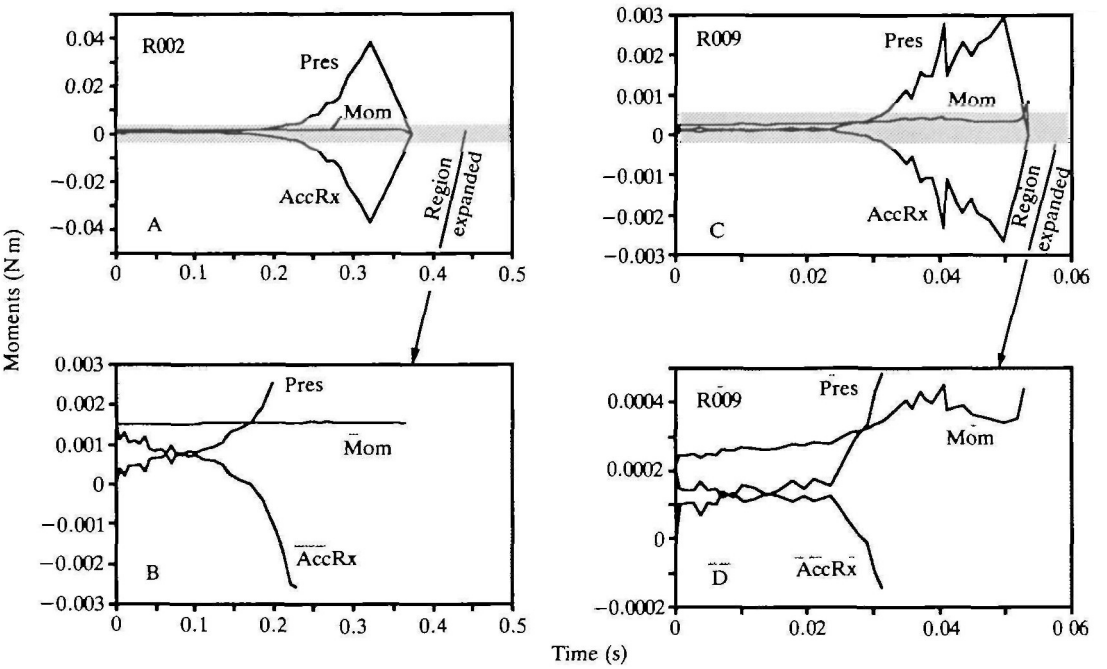

Fig. 7. Magnitude of the closing moment force (Mom), the acceleration reaction (AccRx) and the water pressure force (Pres), during typical closing events, in a Plexiglas model (A,B) and in an empty brachiopod shell (C,D). Models (R002 and R009) are described in Table 1. The vertical scale is expanded in B and D.

forces are (1) the acceleration reaction, related to the acceleration of water from the shell, and (2) pressure forces, which develop as water is expelled from the shell. Fig. 7 shows that the acceleration reaction is large and positive at the initiation of shell closure (corresponding to rapid acceleration of the shell) and large and negative as the shell comes to a close (corresponding to a rapid deceleration of the shell). A positive reaction means that energy is required to accelerate the shell system (shell mass plus added mass of water). A negative reaction, in contrast, means that energy must be extracted from the system to slow it down (the acceleration reaction of a train is very large – difficult to speed up and difficult to slow down).

Calculations indicate that the forces required to accelerate water are of the order of 5–15 times the forces required to accelerate the actual shell model (Table 2). Maximum Reynolds numbers for the tests, which occur at the time of maximum shell-closing velocity, are between 7.1×10^2 and 8.6×10^3 (equation 14 and Table 2).

Fig. 7 shows that high water pressures, as calculated by the hydrodynamic model, are correlated with rapid decelerations of the shell (compare with Figs 3 and 4). Interestingly, at small gapes the calculated water pressures exceed the magnitude of the closing forces, and yet the shell continues to close. This result

could occur because the model is not robust at small gapes (see Results). Alternatively, it is possible that the system's inertia, especially the added inertia of the water, is effectively forcing the shell to close. The system's mass is resisting closure during the initial phases of a closing event, but assisting closure during the later phases of the event. These observations require empirical confirmation by direct measurements (though direct measurements of the acceleration reaction in a rotating inertial system may be very difficult to acquire; T. Daniel, personal communication).

There is a rough correspondence between model predictions and empirical data on actual closing events in brachiopods. For example, data on shell closure in the articulate brachiopod *T. transversa* (S. C. Ackerly, in preparation) indicate that closing times are around 70 ms (time for half-closure is roughly 30 ms), for a shell about 2 cm long and for an initial shell gape of about 0.08 rad (4.5°). Solution of equation 27 for a shell model with these closing characteristics predicts that the mean closing forces on the shell should be about 4.9×10^{-4} N m (5 g cm). Some data on isometric force production in *T. transversa* indicate that peak moments during a twitch contraction of the 'quick' adductor muscles, for a 2 cm long shell, are of the order of 10.8×10^{-4} N m (11 g cm) (S. C. Ackerly, in preparation). If we assume that the time-averaged force is about half this value (a guess), we obtain an observed moment force equal to 5.39×10^{-4} N m (5.5 g cm), which is similar to the predicted value. Observations for the species *Terebratulina retusa*, following a similar argument, give a moment force of about 3.92×10^{-4} N m (4 g cm).

The modeling presented here does not exactly simulate the biological realities observed in living organisms. In living brachiopods, the forces developed during a twitch contraction of the 'quick' adductor muscles are transient and non-steady, whereas in the models the closing force, gravity, is constant and steady. Also, in living brachiopods body tissues occur within the shell and line the shell walls, although the shell gape is not obstructed by mantle tissues as it is in many bivalve molluscs. The diductor muscles, which open the shell, are in direct opposition to the muscles closing the shell. Soft tissues might influence the mechanics of shell closure either by altering the fluid motions as water leaves the shell or by offering resistance (e.g. frictional) to rapid closure (Jaanusson and Neuhaus, 1965). Several lines of evidence suggest that these effects are small. First, the exact pathways of the water are probably less important than the actual mass of water that is accelerated during a closing event. The mass of water accelerated depends primarily on the shell gape and the projected shape of the valves (in a dorsal or ventral view) and not on the configuration of tissues within the shell. Also, Wilkens (1978*b*) reports that the diductor muscles acting in opposition to the adductor muscles possess a remarkable 'slip' mechanism, and tension in this muscle drops suddenly to zero when the muscle is stretched (time interval not specified). Finally, the orientation of the valves might have an effect on the forces required for closure, for example if the brachial valve was above or below the pedicle valve. However, the analysis shows that the mass of the valve is small compared to the mass of water accelerated during a rapid closing event.

Hydrodynamics and skeletal design

Important functions of rapid shell closure are (1) protection of the organism from predators and environmental adversities, and (2) expulsion of material (gametes, feces, detritus) from the shell. From a functional standpoint, protection should be enhanced by maximizing the shell's closing speed, while expulsion functions should be enhanced by maximizing the thrust forces (the product of mass flux and water exit velocity; equation 32). The hydrodynamic model predicts how the closing time and the thrust force depend upon three specific design parameters: (1) the initial shell gape, θ; (2) the closing forces on the shell, M; and (3) shell size, L. For example, the closing time t_c may be expressed by an equation of the form:

$$t_c = e^a L^b M^c \theta^d . \tag{37}$$

where the coefficients a–d are found by regression. The regression is performed on a data matrix representing multiple solutions of equation 27 for different combinations of initial shell gape θ (0.1–0.4 rad), closing force M (1.96×10^{-4}–98×10^{-4} N m or 2–100 g cm) and shell length L (1–5 cm) (statistics package Statview 512+, Macintosh PC). Values of the coefficients a, b, c and d have been derived for the closing time t_c, the time to half-closure $t_{1/2}$, the mean thrust force T_m and the efficiency of thrust production ϵ (Table 4).

The equation for the time to half-closure of the shell:

$$t_{1/2} = e^{-4.7} L^{2.8} M^{-0.50} \theta^{0.001} \tag{38}$$

gives some interesting predictions about the influence of hydrodynamic forces on the performance of the shell-closing mechanism (the time to half-closure $t_{1/2}$ is a better model predictor than the closing time t_c; see above). Interestingly, the initial shell gape has very little effect on the closing time. This result probably reflects the

Table 4. *Dependence of the time for shell closure (t_c, in seconds), the time for half-closure of the shell ($t_{1/2}$, in seconds), the mean propulsive thrust force generated during closure (T_m, in Newtons) and the efficiency of thrust production (ϵ) on shell length (L, in $\times10^{-2}$ m), closing moment (M_s, in g cm) and initial shell gape (θ, in radians), as defined by multiple regression (Statview 512+, Macintosh PC) on results of multiple solutions of the basic hydrodynamic equation, using the mean values of the coefficients, C_p=1.5, J_l=10 (see text)*

	a	b	c	d	r^2	N
t_c	−2.62	2.21	−0.501	0.141	0.999	88
$t_{1/2}$	−4.74	2.81	−0.498	0.001	1.000	88
T_m	−5.88	−0.578	0.999	0.872	0.998	88
ϵ	−0.457	0.440	−0.006	0.023	0.907	88

Relationships of the form: $t_c = e^a L^b M^c \theta^d$.
r is the correlation coefficient and N the size of the data matrix.

relatively large inputs of energy required to accelerate and decelerate the shell, and indicates that these 'costs' are high regardless of the initial shell gape.

Equation 38 also predicts the dependence of the time to half-closure on shell size. If a muscle system scales geometrically, then muscle force (proportional to muscle cross-sectional area) should scale as L^2, and the closing moment ($M=Fd$) should scale as L^3. Substituting $M \propto L^3$ into equation 38 gives the result that the time to half-closure should depend on the length raised to the 1.3 power. In other words, all else being equal, large animals should close more slowly than small animals, thus being at a disadvantage with respect to closing time. A compensatory strategy might be positive allometric growth of the muscle system, i.e. a disproportionate increase in muscle mass, or a shift in muscle position, with increasing shell size (see S. C. Ackerly, in preparation).

The energetic trade-offs between force and speed are difficult to assess. Increasing the muscle mass will, of course, increase the shell's closing speed, but by how much and at what cost? Fig. 8 shows the dependence of the time to half-closure on the closing moment, as predicted by the hydrodynamic model, for shell lengths from 1 to 5 cm. At small forces, the curves have a large negative slope, and small increases in the closing force result in large reductions in the closing time. At larger forces, however, further reductions in the closing time require inordinate increases in the applied moment force. The problem in interpreting these curves is that we must attach specific values to the 'cost of speed' and to the 'cost of force', which are meaningful in terms of an organism's fitness. How fast is fast enough? What forces are 'reasonably' achieved by a brachiopod muscle, and what is the energetic investment of the organism in muscle tissue? These questions can only be resolved by specific case studies. The analysis does, however, suggest that

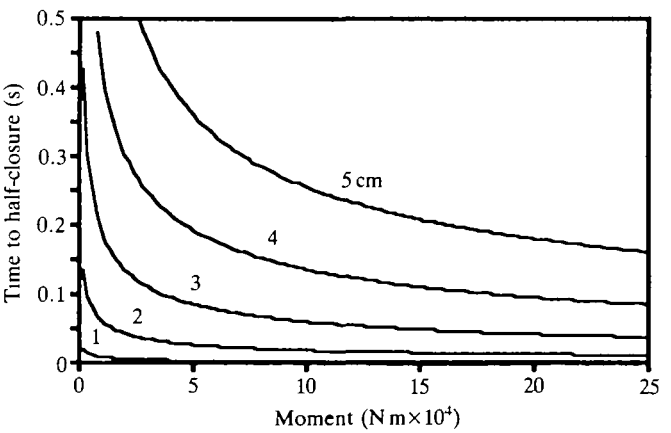

Fig. 8. Dependence of the time to half-closure on the closing moment for different shell sizes (1–5 cm), as predicted, and statistically generalized, by the hydrodynamic model (see text). Increasing the closing force results in reductions in the time to half-closure. Curves are based on an initial shell gape of 0.2 rad.

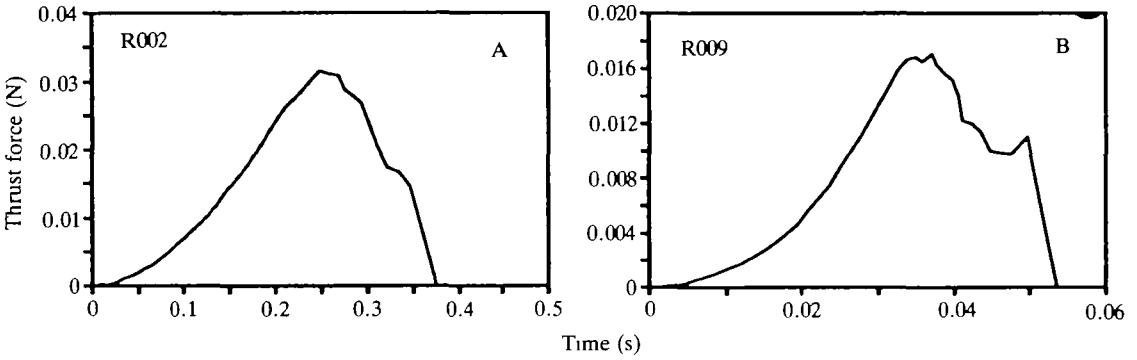

Fig. 9. Calculated magnitudes of the thrust force generated during shell closure. (A) In R002, the static closing force is 0.10 N. (B) In R009, the static closing force is 0.05 N.

there are practical limits to the speeds of shell closure, based on hydrodynamic considerations.

The organism's ability to expel material from the shell can be estimated from the mean thrust generated during a closing event. The direction of the thrust force is not important since the flow is outwards from the shell. The thrust force, calculated as the product of the mass flux of water and the water's exit velocity (equation 32), varies over the course of a closing event (Fig. 9). The mean thrust is found by integration (equation 34) and the efficiency of thrust generation is the ratio of energy inputs to energy outputs (equations 35 and 36, respectively).

The hydrodynamic modeling gives the following dependence of the mean thrust force on shell length, closing force and shell gape (see Table 4):

$$T_m = e^{-5.9} L^{-0.58} M^{1.0} \theta^{0.87}. \quad (39)$$

Equation 39 indicates that the magnitude of the thrust force is directly proportional to the magnitude of the closing force (exponent c=1.0) (i.e. a twofold increase in the closing force results in a twofold increase in the thrust force). Also, increasing the gape apparently permits greater thrust production during a closing event, because more fluid is expelled from the shell during the event. If, as discussed above, the closing moment scales as the third power of shell length, then the thrust forces should increase as the 2.4 power of length.

The efficiency of thrust production is expressed by:

$$\epsilon = e^{-0.46} L^{0.44} M^{-0.006} \theta^{0.02}. \quad (40)$$

From a hydrodynamic standpoint, efficiency increases somewhat with size, but variations in the closing force and initial gape have essentially no effect on the efficiency of thrust production (muscle mechanical considerations might dictate otherwise of course).

Evolutionary implications

In articulate brachiopods, shell closure occurs first by a rapid twitch contraction of the 'quick' adductor muscles, and then by a more prolonged and sustained isometric contraction of the 'catch' adductor muscles. The muscles have separate insertions on the brachial valve and are joined to a common tendon which attaches to the pedicle valve. There is a compelling hydrodynamic argument for the origin of this biphasic muscle system, related to the dependence of water pressure forces on shell gape. Equation 18 for the water pressure force shows that pressure is roughly proportional to the square of the closing velocity and inversely proportional to the square of the shell gape. The inverse dependence of pressure on the shell gape ($1/\theta^2$) indicates that the pressure forces will become very large as the two valves come very close together. There is, in effect, a very high cost of speed at small gapes, involving large expenditures of energy for minimal returns in shell closing speed. The evolutionary development of two muscle systems effectively circumvents this problem of infinite water pressures as the valves occlude. A rapid twitch contraction of the 'quick' adductors produces large transient forces which rapidly close the shell to small gapes. A slower isometric contraction of the 'catch' adductor then takes over to close the shell completely. Hydrodynamic considerations may have contributed to the evolutionary origin of this arrangement of muscles, both in brachiopods and in other taxa (e.g. bivalve molluscs).

Conclusions

Rapid shell closure in articulate brachiopods is subject to fundamental hydrodynamic constraints associated with (1) rapid accelerations of fluid surrounding the shell, and (2) flow velocities of water leaving the shell cavity. A second-order differential equation describing the fluid reactions gives a reasonable first-order approximation of the magnitudes of the inertial and pressure forces developed during a closing event, as observed in shells (with tissues removed) and shell models. The purpose of using models and empty shells is to eliminate the complex, time-dependent forces exhibited by both contractile and non-contractile biological tissues. The hydrodynamic model generates predictions about how variations in shell size, initial shell gape and the closing force influence the history of shell closure. The results provide a quantitative basis for comparative, functional and evolutionary studies in articulate brachiopods.

Appendix

Derivation of the shape constants

Shell size and shape are expressed in terms of the shell's length and a suite of dimensionless shape coefficients that describe characteristics such as shell width, thickness, perimeter, etc. The principal advantage of this approach is that shape and size effects are decoupled from each other. This appendix derives analytical

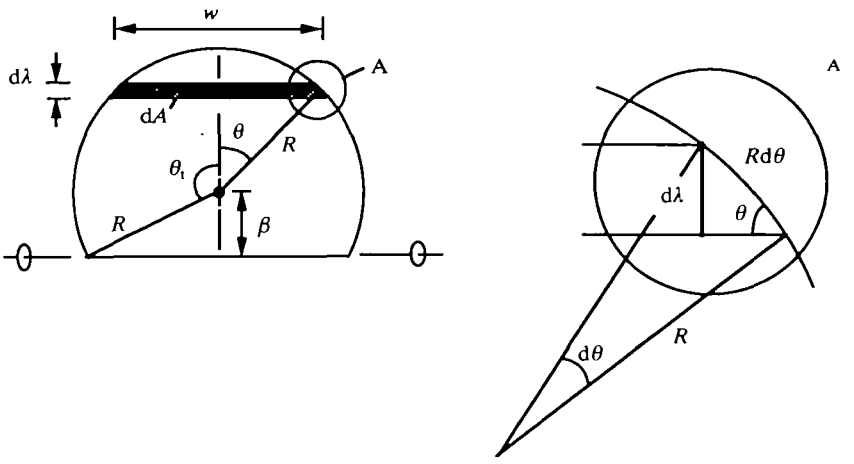

Fig. 10. Geometric parameters for deriving the shape constants. See text for explanation.

expressions for the shape constants, for the idealized geometry represented by the sector of a circle, with radius R, length $R+\beta$, and constant thickness τ (see Fig. 10). Techniques are then described for finding the coefficients of irregularly shaped shells, using (x,y) coordinate data outlining the shell perimeter. The principal requirement is that shape is defined with reference to an axial hinge line, representing the actual shell hinge. Shell shapes are assumed here to be symmetrical with respect to a line bisecting the hinge axis (=median line in brachiopods), but the analysis is easily extended to objects with other symmetries.

Surface area (coefficient: k_w*)*

Idealized geometry

Shell surface area A is the sum of the area increments dA (Fig. 10). The area dA is the product of the width w and length $d\lambda$, so that:

$$dA = w d\lambda. \tag{A1}$$

Expressing w and $d\lambda$ in terms of the radius R and radial position θ gives:

$$w = 2R\sin\theta \tag{A2}$$

and

$$d\lambda = R\sin\theta d\theta, \tag{A3}$$

so that

$$dA = 2R^2 \int \sin^2\theta d\theta \tag{A4}$$

or

$$A = R^2[\theta_t - (\sin^2\theta_t/2)], \tag{A5}$$

where θ_t is the total arc length for the circle segment (Fig. 10). Then, defining

$$A = k_w R^2 \tag{A6}$$

gives

$$k_w = [\theta_t - (\sin^2\theta_t/2)]\,. \tag{A7}$$

For $\theta_t=\pi/2$ (=90°), $k_w=\pi/2$. For $\theta_t=\pi$ (=180°), $k_w=\pi$. The quantity k_wL is the 'equivalent rectangular plate width'.

Irregular geometries

For an irregularly shaped shell defined by (x,y) coordinate pairs along the shell perimeter, where the x axis bisects, and is perpendicular to, the hinge axis and the y axis coincides with the hinge axis, the area is the numerical summation of the area increments dA, so that:

$$A = \Sigma(y_i + y_{i+1})\Delta x\,, \tag{A8}$$

where

$$\Delta x = x_{i+1} - x_i\,, \tag{A9}$$

and

$$k_w = A/L^2\,, \tag{A10}$$

where L is the shell length measured in the x direction.

First moment of area (coefficient: k_a*)*

Idealized geometry

The first moment of area A_1 reflects the distribution of surface area with respect to the hinge axis, so that:

$$A_1 = \int \lambda \mathrm{d}A\,, \tag{A11}$$

where λ is the distance of the area increment dA from the hinge axis. Substituting equations A4 and the relationship:

$$\lambda = \beta + R\cos\theta\,, \tag{A12}$$

where

$$\beta = R\cos(\pi - \theta_t)\,, \tag{A13}$$

into equation A11 gives:

$$A_1 = 2R^3\int[\cos(\pi - \theta_t)\sin^2\theta + \sin^2\theta\cos\theta]\mathrm{d}\theta\,, \tag{A14}$$

or

$$A_1 = \{R^3\cos(\pi - \theta_t)[\theta_t - (\sin^2\theta_t/2)]\} + 2R^3\sin^3\theta_t/3\,. \tag{A15}$$

Setting

$$A_1 = k_a A R\,, \tag{A16}$$

where

$$A = k_w R^2 , \tag{A17}$$

gives

$$k_a = A_1/k_w R^3 . \tag{A18}$$

For $\theta_t=\pi/2$ (=90°), $k_a=4/3\pi$. For $\theta_t=\pi$ (=180°), $k_a=1$.

Irregular geometries

The first moment of area in terms of (x,y) coordinate pairs is:

$$A_1 = \Sigma[(y_i + y_{i+1})(x_i + x_{i+1})\Delta x/2] , \tag{A19}$$

so that:

$$k_a = A_1/AL^2 . \tag{A20}$$

First moment of perimeter (coefficient: k_{ex}*)*

Idealized geometry

The first moment of perimeter reflects the distribution of perimeter segments dp with respect to the hinge, so that:

$$p_1 = \int \lambda \mathrm{d}p , \tag{A21}$$

where

$$\mathrm{d}p = R\mathrm{d}\theta . \tag{A22}$$

Thus:

$$p_1 = 2R^2 \int [\cos(\pi - \theta_t) + \cos\theta]\mathrm{d}\theta , \tag{A23}$$

or

$$p_1 = 2R^2[\theta_t \cos(\pi - \theta_t) + \sin\theta_t] . \tag{A24}$$

Defining

$$p_1 = k_p p R , \tag{A25}$$

where

$$p = k_l R , \tag{A26}$$

gives the expression for k_p:

$$k_p = p_1/(k_l R^2) , \tag{A27}$$

where k_p is a coefficient of the first moment of perimeter. I also define the coefficient k_{ex} as a coefficient of the first moment of perimeter, where:

$$\begin{aligned} k_{ex} &= k_p k_l , \\ &= p_i/R^2 . \end{aligned} \tag{A28}$$

For $\theta_t=\pi/2$ (=90°), $k_{ex}=2$. For $\theta_t=\pi$ (=180°), $k_{ex}=2\pi$.

Irregular geometries

The first moment of perimeter in terms of (x,y) coordinate pairs is:

$$p_1 = \Sigma[(\Delta y^2 + \Delta x^2)/2(x_i + x_{i+1})]\,, \tag{A29}$$

so that:

$$k_{ex} = p_1/L^2\,. \tag{A30}$$

First moment of inertia (coefficient: k_{cm})

Idealized geometry

The first moment of inertia M_1 reflects the distribution of volume with respect to the hinge axis. For a shell of constant thickness, the coefficient of the first moment of inertia k_{cm} is equal to the coefficient of the first moment of area k_a.

Irregular geometries

For irregular geometries, where the shell thickness varies in both the x and y directions, numerical calculations become laborious, and empirical methods are preferred. One technique for measuring the distribution of volume, assuming a shell of constant density, is to suspend the shell by a wire, hinge uppermost, on a balance, and to lower the shell by successive increments into a beaker of water, recording the mass of the shell at each stage. The relative mass reduction at each stage gives the relative volume of the shell for that increment, which is standardized against the total volume.

Second moment of inertia (coefficient: J_b)

Idealized geometry

The second moment of inertia M_2 reflects the distribution of volume with respect to the hinge axis, so that:

$$M_2 = \int \lambda^2 dV\,, \tag{A31}$$

where, for constant shell thickness τ,

$$dV = \tau dA\,. \tag{A32}$$

Defining

$$\tau = k_t R\,, \tag{A33}$$

and by the relationships defined above:

$$M_2 = 2k_t R^5 \int [\cos^2(\pi - \theta_t)\sin^2\theta + \cos(\pi - \theta_t)\sin^2\theta\cos\theta + \sin^2\theta\cos^2\theta]d\theta \tag{A34}$$

or

$$M_2 = k_t R^5 \{\cos^2(\pi - \theta)[\theta - (\sin 2\theta)]/4 + 2\cos(\pi - \theta)\sin^3\theta/3 + \theta/4 - \sin 4\theta/16\}\,, \quad \text{(A35)}$$

where $\theta = \theta_t$. Setting:

$$M_2 = J_b V R^3\,, \quad \text{(A36)}$$

gives

$$J_b = M_2/k_w k_t R^5\,. \quad \text{(A37)}$$

For $\theta_t = \pi/2$ (so $k_w = \pi/2$, for a semi-circle), $J_b = 0.5$.

List of symbols

Symbol	Quantity	Units
a	Linear acceleration	$m\,s^{-2}$
a_f	Linear acceleration of external load	$m\,s^{-2}$
a_l	Acceleration of water leaving shell	$m\,s^{-2}$
A	Surface area of the shell	m^2
A_1	First moment of area	–
A_m	Cross-sectional area of the muscle	cm^2
A_{ex}	Exit area	m^2
A_s	Surface area	m^2
C_p, C_p*	Pressure coefficient	–
d	Moment arm distance	m
d_f	Position of external load	m
e	Natural logarithm base=2.718	–
E_i	Energy inputs	$kg\,m^2\,s^{-2}$
E_o	Energy outputs	$kg\,m^2\,s^{-2}$
F	Force	$kg\,m\,s^{-2}$
g	Gravitational constant ($9.8\,m\,s^{-2}$)	–
I_b	Inertia of body	$kg\,m^2$
I_l	Inertia of liquid	$kg\,m^2$
J_b	Coefficient of inertia of body	–
J_l	Coefficient of inertia of liquid	–
k_a	Coefficient of first moment of area	–
k_{cm}	Coefficient of center of mass	–
k_{cp}	Coefficient of center of pressure	–
k_{ex}, k_p	Coefficients of first moment of perimeter	–
k_l	Coefficient of perimeter	–
k_t	Coefficient of thickness	–
k_w	Coefficient of width	–
K_{1-4}	Generic coefficients	–

L	Length	m
m	Mass	kg
m_b	Mass of the shell	kg
m_f	Mass of external loads	kg
M	Moment force	N m
M_1	First moment of inertia	–
M_2	Second moment of inertia	–
M_b	Gravitational moment of body	N m
M_f	Gravitational moment of external loads	N m
M_g	Closing forces due to gravity	N m
M_p	Moment force due to pressure	N m
M_s	Static closing moment force	g cm
p	Perimeter	cm
p_1	First moment of perimeter	–
P	Pressure	$N\,m^{-2}$
R	Shell radius	cm
Re	Reynolds number	–
t	Time	s
t_c	Closing time	s
$t_{1/2}$	Time for half closure	s
$t_{\omega max}$	Time of maximum velocity	s
T	Thrust force	$kg\,m\,s^{-2}$
T_m	Mean thrust force	$kg\,m\,s^{-2}$
u	Velocity	$m\,s^{-1}$
u_l	Mean exit velocity of liquid	$m\,s^{-1}$
v	Muscle contraction velocity	$m\,s^{-1}$
V	Volume	m^3
V_b	Volume of shell material	–
w	Width of shell increment	cm
α	Angular acceleration	$rad\,s^{-2}$
β	Fraction of the shell radius	cm
γ	Added mass coefficient	–
∂	Error term	–
ϵ	Efficiency	–
λ	Length in a direction normal to hinge	cm
ν	Kinematic viscosity	$m^2\,s^{-1}$
π	Constant=3.14159	–
θ	Angular position	rad
θ_t	Arc length of a circle segment	rad
ρ	Density	$kg\,m^{-3}$
ρ_b	Density of the shell	$kg\,m^{-3}$
ρ_l	Density of the fluid	$kg\,m^{-3}$
τ	Shell thickness	mm
ω	Angular velocity	$rad\,s^{-1}$

I wish to thank Professors J. Cisne, T. Daniel, M. LaBarbera, K. Niklas, S. Vogel and A. McCune for critical and helpful discussions. The comments of two anonymous reviewers resulted in significant improvements to the manuscript.

References

DANIEL, T. L. (1983). Mechanics and energetics of medusan jet propulsion. *Can. J. Zool.* **61**, 1406–1420.

DANIEL, T. L. (1984). Unsteady aspects of aquatic locomotion. *Am. Zool.* **24**, 121–134.

JAANUSSON, V. AND NEUHAUS, H. (1965). Mechanism of the diductor muscles in articulate brachiopods. *Stockholm Contributions in Geology* **13**, 1–8.

RUDWICK, M. J. S. (1961). 'Quick' and 'catch' adductor muscles in brachiopods. *Nature* **191**, 1021.

SAUNDERS, H. E. (1957). *Hydrodynamics in Ship Design*. vol. 1, 648pp. vol. 2, 980pp. New York: Society of Naval Architects and Marine Engineers.

WILKENS, J. L. (1978*a*). Adductor muscles of brachiopods: activation and contraction. *Can. J. Zool.* **56**, 315–323.

WILKENS, J. L. (1978*b*). Diductor muscles of brachiopods: activation and very slow contraction. *Can. J. Zool.* **56**, 324–332.